Hybrid Vlasov-MHD models: Hamiltonian vs. non-Hamiltonian

2014 Plasma Phys. Control. Fusion 56 095008

(http://iopscience.iop.org/0741-3335/56/9/095008)

IOP Publishing | Plasma Physics and Controlled Fusion

Plasma Phys. Control. Fusion **56** (2014) 095008 (11pp) doi:10.1088/0741-3335/56/9/095008

Hybrid Vlasov-MHD models: Hamiltonian vs. non-Hamiltonian

Cesare Tronci[1], **Emanuele Tassi**[2], **Enrico Camporeale**[3] **and Philip J Morrison**[4]

[1] Department of Mathematics, University of Surrey, Guildford GU2 7XH, UK
[2] CNRS & Centre de Physique Théorique, Campus de Luminy, 13288 Marseille cedex 9, France and Université de Toulon, CNRS, CPT, UMR 7332, 83957, La Garde, France
[3] Centrum Wiskunde & Informatica, 1098 XG Amsterdam, The Netherlands
[4] Department of Physics & Institute for Fusion Studies, University of Texas, Austin, TX 78712-0262, USA

E-mail: c.tronci@surrey.ac.uk, emanuele.tassi@cpt.univ-mrs.fr, e.camporeale@cwi.nl and morrison@physics.utexas.edu

Received 1 March 2014, revised 24 May 2014
Accepted for publication 12 June 2014
Published 8 July 2014

Abstract

This paper investigates hybrid kinetic-magnetohydrodynamic (MHD) models, where a hot plasma (governed by a kinetic theory) interacts with a fluid bulk (governed by MHD). Different nonlinear coupling schemes are reviewed, including the pressure-coupling scheme (PCS) used in modern hybrid simulations. This latter scheme suffers from being non-Hamiltonian and is unable to exactly conserve total energy. Upon adopting the Vlasov description for the hot component, the non-Hamiltonian PCS and a Hamiltonian variant are compared. Special emphasis is given to the linear stability of Alfvén waves, for which it is shown that a spurious instability appears at high frequency in the non-Hamiltonian version. This instability is removed in the Hamiltonian version.

Keywords: magnetohydrodynamics, Vlasov equation, hybrid kinetic-MHD

(Some figures may appear in colour only in the online journal)

1. Introduction

Several configurations in plasma physics involve the interaction of a hot plasma species with a lower temperature bulk component. Typical examples are those of nuclear fusion devices, in which the energetic alpha particles produced by the fusion reactions interact with the ambient plasma, and those of space plasmas, involving the interaction between the energetic solar wind and Earth's magnetosphere. Such plasmas have been studied for decades and yet continue to be the subject of current research.

For such configurations, one is first interested in ascertaining the stabilizing or destabilizing effects that the energetic component can have on the overall system. In order to address this question, various mathematical models have been formulated to include the combined effects of both the energetic particles and the bulk plasma. Although the bulk can be well described by ordinary magnetohydrodynamics (MHD), adequately modeling the hot species requires the use of kinetic theory. This multiscale, multi-physics approach leads to the formulation of hybrid kinetic-MHD models that couple the MHD equations to a kinetic equation for the hot component. Then, the question of which kinetic equation to use for the hot particles arises. Typically drift-kinetic, gyrokinetic, or the full Vlasov system are used. In plasma fusion, the first two options are used most often, while the full Vlasov description is needed for e.g. reverse field pinch plasmas [11]. The full Vlasov description solves for effects at all scales and thus is less convenient when the hot particle gyromotion can be averaged out, in favor of drift-kinetic and gyrokinetic models. Nevertheless, this paper aims to account for hot particle effects at all possible scales, so that the full Vlasov description is adopted.

Another more important question emerges in the formulation of hybrid kinetic-MHD models, viz., the particular type of coupling scheme that should be used in the model. Two coupling schemes are present in the literature: the current-coupling scheme (CCS), found for example in [1, 3, 30] and the pressure-coupling scheme (PCS), examples of which are used in [4, 7, 12]. While the CCS involves the hot momentum and density

$$\boldsymbol{K} = \int \boldsymbol{p}\, f(\boldsymbol{x}, \boldsymbol{p})\, \mathrm{d}^3\boldsymbol{p}, \tag{1}$$

$$n = \int f(\boldsymbol{x}, \boldsymbol{p})\, \mathrm{d}^3\boldsymbol{p}, \tag{2}$$

the PCS involves the following tensor:

$$\mathbb{P} = \frac{1}{m_h} \int \boldsymbol{p}\boldsymbol{p}\, f(\boldsymbol{x}, \boldsymbol{p})\, \mathrm{d}^3\boldsymbol{p}, \tag{3}$$

which is the pressure tensor of the hot component, calculated with respect to a zero mean velocity. All these quantities are defined as above in terms of moments of the kinetic probability density $f(\boldsymbol{x}, \boldsymbol{p})$ on phase space. Here, $\boldsymbol{p}$ denotes the kinetic momentum $\boldsymbol{p} = m_h \boldsymbol{v}$, while m_h denotes the hot particle mass. Normally, the PCS is derived from the CCS [24, 25], under the assumption that the hot component is rarefied, so that its density levels are much lower than those of the MHD component. Also, the PCS often appears in two different versions depending on whether the definition of the pressure tensor involves the absolute [4, 7] or relative [12, 29] velocity.

All of the nonlinear PCS models commonly found in plasma physics literature suffer from the defect that they do not exactly conserve energy. Indeed, exact energy conservation is lost when the assumption of a rarefied hot component is inserted as an approximation in the equations of motion of the model. Consequently, these models are not Hamiltonian field theories, ones that are expected to have noncanonical Poisson brackets akin to those introduced into plasma physics in [21] for MHD and [19, 20] for the Vlasov equation. Since such a Hamiltonian structure occurs for all good plasma models, in their non-dissipative limit, (see [16, 17, 19]), this would suggest there should be a Hamiltonian model for the PCS, and indeed this was shown to be the case in recent literature [10, 23, 31]. This new model not only conserves energy, but also conserves the cross-helicity invariants (which are also lost in the non-Hamiltonian case).

A main goal of the present paper is to compare the Hamiltonian and non-Hamiltonian PCS models, with emphasis on linear stability analyses. It is important to make clear that we are not arguing that dissipation is unimportant and that the Hamiltonian description is the most apt description of hybrid plasmas; clearly this is not always the case—collisional effects, albeit small, can give rise to important consequences, as is evident, for instance, from the massive body of reconnection studies in the literature. Rather, the goal here is to investigate some consequences of nonphysical dissipation (or drive) that exists in hybrid models when all the clearly identifiable physical dissipative terms are set to zero. This fake dissipation may also be small, as is often the case for physical dissipation, but could lead to substantial yet erroneous consequences. Indeed, we discover a spurious instability in the non-Hamiltonian model.

The remainder of the paper is organized as follows. In section 2 we review the two hybrid coupling schemes: the CCS and PCS models are derived from first principles and general comments about their structure are made. This is followed in section 3 by a general treatment of the linear problem for the incompressible PCS models expanded about homogeneous isotropic equilibria in a uniform external magnetic field, by integration over orbits. This is followed, in section 4, by a study of the dispersion relation for transverse disturbances parallel to the magnetic field. It is in this special case that we compare the Hamiltonian and non-Hamiltonian PCS models and discover the spurious instability. For completeness we also compare them to the CCS models. The dispersion relation is analyzed numerically and analytically and is shown to have a crossover to instability at high frequencies. Next, in section 5, comments are made about the behavior of perpendicular disturbances. Finally, in section 6 we summarize and conclude. The paper contains two appendices that are included for completeness. In appendix A the noncanonical Poisson brackets for the Hamiltonian hybrid models are given, while appendix B records some details of our calculations leading to the dispersion relation used in section 4.

2. Hybrid coupling schemes

Turning now to the two coupling schemes, we first consider the CCS, then the PCS.

2.1. Current-coupling schemes

In order to derive the hybrid CCS model [25], one starts with the equations of motion for a multifluid plasma in the presence of an energetic component. Upon formally neglecting the vacuum permittivity (see e.g. [5]), one writes

$$\begin{aligned} \rho_s \left(\frac{\partial \boldsymbol{u}_s}{\partial t} + \boldsymbol{u}_s \cdot \nabla \boldsymbol{u}_s \right) &= -\nabla \mathsf{p}_s \\ &\quad + \rho_s a_s \left(\boldsymbol{E} + \boldsymbol{u}_s \times \boldsymbol{B} \right), \end{aligned} \tag{4}$$

$$\frac{\partial \rho_s}{\partial t} + \nabla \cdot (\rho_s \boldsymbol{u}_s) = 0, \tag{5}$$

$$\frac{\partial f}{\partial t} + \frac{\boldsymbol{p}}{m_h} \cdot \frac{\partial f}{\partial \boldsymbol{x}} + q_h \left(\boldsymbol{E} + \frac{\boldsymbol{p}}{m_h} \times \boldsymbol{B} \right) \cdot \frac{\partial f}{\partial \boldsymbol{p}} = 0,$$

$$\begin{aligned} \nabla \times \boldsymbol{B} &= \mu_0 \boldsymbol{J} \\ &= \mu_0 \sum_s a_s \rho_s \boldsymbol{u}_s + \mu_0\, a_h \boldsymbol{K}, \end{aligned} \tag{6}$$

$$\frac{\partial \boldsymbol{B}}{\partial t} = -\nabla \times \boldsymbol{E}, \tag{7}$$

$$0 = \sum_s a_s \rho_s + q_h n, \qquad \nabla \cdot \boldsymbol{B} = 0, \tag{8}$$

where $a_s = q_s/m_s$ is the charge-to-mass ratio for the fluid species s, while ρ_s and $\boldsymbol{u}_s$ are its mass density and velocity, respectively. The symbol p_s, on the other hand, indicates the partial pressure of the fluid species s, which is assumed to be a function of ρ_s, through the relation $\mathsf{p}_s = \rho_s^2 \partial \mathcal{U}_s/\partial \rho_s$, with $\mathcal{U}_s(\rho_s)$ indicating the corresponding specific internal energy.

For simplicity, we consider from now on, the case in which the bulk plasma is composed by two species, one consisting of ions and the second one of electrons. It is customary to reduce the two-fluid system by neglecting the inertia of the electron species (taking the limit $m_2 \to 0$), thereby obtaining a one-fluid momentum equation. With this assumption, summation of equations (4) for $s = 1, 2$ produces

$$\rho_1 \left(\frac{\partial \boldsymbol{u}_1}{\partial t} + \boldsymbol{u}_1 \cdot \nabla \boldsymbol{u}_1 \right) = (a_1\rho_1 + a_2\rho_2)\, \boldsymbol{E} + (a_1\rho_1\boldsymbol{u}_1 + a_2\rho_2\boldsymbol{u}_2) \times \boldsymbol{B} - \nabla \mathsf{p}\,, \tag{9}$$

where $\mathsf{p} = \mathsf{p}_1 + \mathsf{p}_2$. Then, upon using Ampère's law (6) and the quasineutrality relation of (8), equation (9) becomes

$$\rho_1 \left(\frac{\partial \boldsymbol{u}_1}{\partial t} + \boldsymbol{u}_1 \cdot \nabla \boldsymbol{u}_1 \right) = -q_h n \boldsymbol{E} + (\boldsymbol{J} - a_h \boldsymbol{K}) \times \boldsymbol{B} - \nabla \mathsf{p}, \tag{10}$$

while equation (4) for the second species yields

$$\boldsymbol{E} = -\boldsymbol{u}_2 \times \boldsymbol{B} + \frac{1}{a_2\rho_2} \nabla \mathsf{p}_2 = \frac{1}{a_2\rho_2} (a_1\rho_1\boldsymbol{u}_1 + a_h\boldsymbol{K} - \boldsymbol{J}) \times \boldsymbol{B} + \frac{1}{a_2\rho_2} \nabla \mathsf{p}_2.$$

Next, one imitates the derivation of ideal MHD [5] and assumes that $\boldsymbol{J} \times \boldsymbol{B}$ and $\nabla \mathsf{p}_2$ are both negligible compared to the Lorentz force $a_1\rho_1\boldsymbol{u}_1 \times \boldsymbol{B}$. This step leads to an Ohm's law of the form

$$\boldsymbol{E} = -\left(\frac{a_1\rho_1\boldsymbol{u}_1 + q_h n \boldsymbol{V}}{a_1\rho_1 + q_h n} \right) \times \boldsymbol{B}, \tag{11}$$

where $\boldsymbol{V} = m_h^{-1}\boldsymbol{K}/n$ is the hot mean velocity. Note, this means magnetic flux is frozen-in at a velocity given by

$$\boldsymbol{W} = \frac{a_1\rho_1\boldsymbol{u}_1 + q_h n \boldsymbol{V}}{a_1\rho_1 + q_h n}. \tag{12}$$

However, if $\boldsymbol{V}$ and $\boldsymbol{u}_1$ are comparable and $a_1\rho_1 \gg q_h n_h$, then one can replace (11) by the Ohm's law of ideal MHD,

$$\boldsymbol{E} = -\boldsymbol{u}_1 \times \boldsymbol{B}, \tag{13}$$

and the magnetic flux is then frozen into the MHD bulk flow. Finally, inserting (13) into equations (10), (5), and (7) yields the Hamiltonian CCS:

$$\rho \left(\frac{\partial \boldsymbol{u}}{\partial t} + \boldsymbol{u} \cdot \nabla \boldsymbol{u} \right) = -\nabla \mathsf{p} + (q_h n \boldsymbol{u} - a_h \boldsymbol{K} + \boldsymbol{J}) \times \boldsymbol{B}, \tag{14}$$

$$\frac{\partial \rho}{\partial t} + \nabla \cdot (\rho \boldsymbol{u}) = 0, \tag{15}$$

$$\frac{\partial f}{\partial t} + \frac{\boldsymbol{p}}{m_h} \cdot \frac{\partial f}{\partial \boldsymbol{x}} + q_h \left(\frac{\boldsymbol{p}}{m_h} - \boldsymbol{u} \right) \times \boldsymbol{B} \cdot \frac{\partial f}{\partial \boldsymbol{p}} = 0, \tag{16}$$

$$\frac{\partial \boldsymbol{B}}{\partial t} = \nabla \times (\boldsymbol{u} \times \boldsymbol{B})\,, \tag{17}$$

where the subscript 1 has been dropped. The system (14)–(17) is identical to the current-coupling hybrid scheme presented in [1, 3, 25], except for the fact that the hot particle dynamics is governed by the Vlasov equation rather than gyrokinetic or drift-kinetic counterparts.

Note, we always assume that the mean velocity $\boldsymbol{V} = m_h^{-1}\boldsymbol{K}/n$ of the energetic component is either very low or at most comparable with the MHD fluid velocity $\boldsymbol{u}$. This is consistent with the hypothesis of energetic particles, since the latter hypothesis involves the temperature rather than the mean velocity. Denoting the temperatures of the hot and fluid components by T_h and T_f, respectively, we have $T_h \gg T_f$ (see [4]). With the definition of the temperature $T_h = (m_h/3nk_B)\int |\boldsymbol{v} - \boldsymbol{V}|^2 f\, \mathrm{d}^3\boldsymbol{v}$ (where k_B denotes Boltzmann's constant), the assumption on the energetic component amounts to an assumption on the trace of the second-order moment of the Vlasov density with no assumption on the mean velocity, which is actually low for hot particles close to isotropic equilibria [29].

Notice that equation (14) involves the Lorentz force term $q_h n \boldsymbol{u} \times \boldsymbol{B}$, which should normally be negligible for consistency with the approximation $m_h n \ll \rho$, which yields equation (13) from equation (11). A variant of the above CCS also exists [30], which, by virtue of the approximation $m_h n \ll \rho$ neglects the term $q_h n \boldsymbol{u} \times \boldsymbol{B}$, but on the other hand retains the term $\boldsymbol{K} \times \boldsymbol{B}$ even though the two terms are in principle of the same order (as long as $\boldsymbol{V}$ is comparable with $\boldsymbol{u}$).

One can check directly that the hybrid CCS model of (14)–(17) exactly conserves the following total energy:

$$\mathcal{E} = \frac{1}{2}\int \rho |\boldsymbol{u}|^2 \mathrm{d}^3\boldsymbol{x} + \frac{1}{2m_h}\int f\, |\boldsymbol{p}|^2\, \mathrm{d}^3\boldsymbol{x}\, \mathrm{d}^3\boldsymbol{p} + \int \rho\, \mathcal{U}(\rho)\, \mathrm{d}^3\boldsymbol{x} + \frac{1}{2\mu_0}\int |\boldsymbol{B}|^2\, \mathrm{d}^3\boldsymbol{x}, \tag{18}$$

(see [30]) where $\mathcal{U}(\rho)$ is the internal energy per unit mass, from which the pressure is determined by $\mathsf{p} = \rho^2 \partial \mathcal{U}/\partial \rho$. Moreover, this system is Hamiltonian, with a noncanonical Poisson bracket [31] (recorded for completeness in appendix A) and it conserves the usual cross-helicity invariant $\int \boldsymbol{u} \cdot \boldsymbol{B}\, \mathrm{d}^3\boldsymbol{x}$ [10].

2.2. *Pressure-coupling schemes*

Let us consider now the two models that use the PCS—first the non-Hamiltonian version then the Hamiltonian one.

2.2.1. Non-Hamiltonian PCS. Once the CCS has been obtained, the PCS can be derived by computing the evolution of the total momentum

$$\boldsymbol{M} := \rho \boldsymbol{u} + \boldsymbol{K} =: \rho \boldsymbol{U}, \tag{19}$$

which gives (cf equation (1) of [25])

$$\frac{\partial \boldsymbol{K}}{\partial t} + \rho \left(\frac{\partial \boldsymbol{u}}{\partial t} + \boldsymbol{u} \cdot \nabla \boldsymbol{u} \right) = -\nabla \cdot \mathbb{P} - \nabla \mathsf{p} + \boldsymbol{J} \times \boldsymbol{B}. \tag{20}$$

Since $\partial_t \boldsymbol{K} = \rho\, \partial_t(\boldsymbol{K}/\rho) + (\mathrm{div}\boldsymbol{u})\boldsymbol{K}/\rho$, inserting the assumption $\boldsymbol{K}/\rho \ll \boldsymbol{u}$ yields

$$\rho \left(\frac{\partial \boldsymbol{U}}{\partial t} + \boldsymbol{u} \cdot \nabla \boldsymbol{u} \right) = -\nabla \cdot \mathbb{P} - \nabla \mathsf{p} + \boldsymbol{J} \times \boldsymbol{B}. \tag{21}$$

Then, upon writing $\boldsymbol{U} \sim \boldsymbol{u}$, we obtain the system with the non-Hamiltonian PCS:

$$\rho\left(\frac{\partial \boldsymbol{U}}{\partial t}+\boldsymbol{U}\cdot\nabla\boldsymbol{U}\right)=-\nabla\mathsf{p}-\nabla\cdot\mathbb{P}+\boldsymbol{J}\times\boldsymbol{B} \tag{22}$$

$$\frac{\partial\rho}{\partial t}+\nabla\cdot(\rho\boldsymbol{U})=0 \tag{23}$$

$$\frac{\partial f}{\partial t}+\frac{\boldsymbol{p}}{m_h}\cdot\frac{\partial f}{\partial \boldsymbol{x}}+q_h\left(\frac{\boldsymbol{p}}{m_h}-\boldsymbol{U}\right)\times\boldsymbol{B}\cdot\frac{\partial f}{\partial \boldsymbol{p}}=0 \tag{24}$$

$$\frac{\partial \boldsymbol{B}}{\partial t}=\nabla\times(\boldsymbol{U}\times\boldsymbol{B}), \tag{25}$$

Notice that equation (22) is identical to the bulk momentum equation of the hybrid PCS of Fu and Park (see equation (1) in [7, 8]), which also includes (23) and (25) (while replacing Vlasov dynamics by its gyrokinetic approximation). Analogous PCS models with the same fluid equation (22) have been formulated by Cheng [4] (see equation (1) therein) and Park *et al* [25] (see equation (3) therein). In some situations, the tensor (3) in (22) is replaced by the relative pressure tensor $\widetilde{\mathbb{P}} = m_h^{-1}\int(\boldsymbol{p}-m_h\boldsymbol{V})(\boldsymbol{p}-m_h\boldsymbol{V})f\,\mathrm{d}^3\boldsymbol{p}$ (e.g., the PCS model proposed by Kim, Sovinec and Parker [11, 12, 29]).

All the above mentioned PCS models suffer from not exactly conserving the total energy. Indeed, if we assume that the total energy is still given by (18), equations (22)–(25) give $\dot{\mathcal{E}} = \int \boldsymbol{U}\cdot\partial_t\boldsymbol{K}\,\mathrm{d}^3\boldsymbol{x}$, so that the total energy would only be nearly conserved if $\partial_t\boldsymbol{K}$ is small. Under this assumption, the CCS and the PCS are completely equivalent, since (16) yields

$$\frac{\partial\boldsymbol{K}}{\partial t}=-\nabla\cdot\mathbb{P}+a_h\boldsymbol{K}\times\boldsymbol{B}-q_hn\boldsymbol{u}\times\boldsymbol{B}. \tag{26}$$

However, the assumption that $\partial_t\boldsymbol{K}$ is negligible is *not* compatible with (16), since the time variation of $\boldsymbol{K}$ may indeed play a role in the general case.

2.2.2. Hamiltonian PCS. The issue of exact energy conservation was raised in [31], where an alternative Hamiltonian version of the PCS was presented. Besides conserving the energy (18) exactly, this model possesses a Poisson bracket structure, which was derived by using well established Hamiltonian techniques in geometric plasma dynamics [14–21, 27, 28].

In order to derive the Hamiltonian PCS model of [31], one expresses the Hamiltonian structure of the CCS (14)–(17) in terms of the total momentum $\boldsymbol{M}$ in (19). Then, instead of replacing $\boldsymbol{U} \sim \boldsymbol{u}$ (arising from the original assumption $m_hn \ll \rho$) in the equations of motion, one replaces $\boldsymbol{U} \sim \boldsymbol{u}$ directly in (18) and derives the equations of motion from the Poisson bracket structure written in terms of $\boldsymbol{M}$ (see appendix A). This procedure ensures that the chosen energy functional is always preserved, as long as no approximations are made on the Poisson bracket. At this point, one obtains the following set of equations for the Hamiltonian PCS:

$$\rho\left(\frac{\partial \boldsymbol{U}}{\partial t}+\boldsymbol{U}\cdot\nabla\boldsymbol{U}\right)=-\nabla\mathsf{p}-\nabla\cdot\mathbb{P}+\boldsymbol{J}\times\boldsymbol{B} \tag{27}$$

$$\begin{aligned}\frac{\partial f}{\partial t}&+\left(\frac{\boldsymbol{p}}{m_h}+\boldsymbol{U}\right)\cdot\frac{\partial f}{\partial \boldsymbol{x}}\\&+\Big[\boldsymbol{p}\times\left(a_h\boldsymbol{B}-\nabla\times\boldsymbol{U}\right)-\boldsymbol{p}\cdot\nabla\boldsymbol{U}\Big]\cdot\frac{\partial f}{\partial \boldsymbol{p}}=0,\end{aligned} \tag{28}$$

$$\frac{\partial\rho}{\partial t}+\nabla\cdot(\rho\,\boldsymbol{U})=0,\qquad \frac{\partial \boldsymbol{B}}{\partial t}=\nabla\times(\boldsymbol{U}\times\boldsymbol{B}). \tag{29}$$

We see that the fluid equation (27) is identical to the corresponding equation (22) of the non-Hamiltonian model. However, in the Hamiltonian model, hot particles move with the relative velocity $\boldsymbol{U}+\boldsymbol{p}/m_h$ so that the term $\nabla\boldsymbol{U}\cdot\boldsymbol{p} = \boldsymbol{p}\cdot\nabla\boldsymbol{U}+\boldsymbol{p}\times(\nabla\times\boldsymbol{U})$ appears as an inertial force. Consequently, both Hamiltonian and non-Hamiltonian PCS' possess the same static equilibria, although the dynamics in the vicinity of these equilibria may be very different, depending on the particular situation under consideration. Also, we notice that, unlike the CCS of (14)–(17) and the non-Hamiltonian PCS of (22)–(25), the Hamiltonian equations of (27)–(29) involve a nontrivial kinetic-fluid coupling, even in the absence of magnetic fields.

3. Linearized incompressible PCS

In this section, we consider the linearized equations of motion for the incompressible limit (e.g. $\nabla\cdot\boldsymbol{U} = 0$) of both Hamiltonian and non-Hamiltonian PCS'. For the sake of simplicity, we shall set all physical constants to unity (including m_h, so that $\boldsymbol{p} = \boldsymbol{v}$), although we shall restore them at a later time.

3.1. Equations of motion

Upon following the standard procedure, we linearize each variable as $A = A_0 + A_1$, so that the subscripts '0' and '1' denote an equilibrium and its perturbation, respectively. As a result, we obtain

$$\frac{\partial \boldsymbol{U}_1}{\partial t}=-\nabla\mathsf{p}_1-\nabla\cdot\int\boldsymbol{v}\boldsymbol{v}f_1\,\mathrm{d}^3\boldsymbol{v}+(\nabla\times\boldsymbol{B}_1)\times\boldsymbol{B}_0, \tag{30}$$

$$\begin{aligned}\frac{\partial f_1}{\partial t}&+\boldsymbol{v}\cdot\frac{\partial f_1}{\partial \boldsymbol{x}}+\boldsymbol{v}\times\boldsymbol{B}_0\cdot\frac{\partial f_1}{\partial \boldsymbol{v}}\\&=f_0'\left(\alpha\boldsymbol{v}\boldsymbol{v}:\nabla\boldsymbol{U}_1+\beta\boldsymbol{v}\cdot\boldsymbol{U}_1\times\boldsymbol{B}_0\right),\end{aligned} \tag{31}$$

$$\frac{\partial \boldsymbol{B}_1}{\partial t}=\nabla\times(\boldsymbol{U}_1\times\boldsymbol{B}_0),\qquad \nabla\cdot\boldsymbol{U}_1=0, \tag{32}$$

where the parameters α and $\beta = 1-\alpha$ are inserted so that $\alpha = 1$ gives the linearized Hamiltonian model, while $\alpha = 0$ gives the linearized non-Hamiltonian model. In this way, it is clear that the α-terms identify the Hamiltonian model, while the β-terms identify its non-Hamiltonian counterpart. In equations (30)–(32) we assumed a static equilibrium so that $\boldsymbol{U}_0 \equiv 0$ and $\mathsf{p}_0 \equiv 0$. Also, we consider a uniform magnetic field $\boldsymbol{B}_0$ (aligned with the z-axis) and an isotropic equilibrium for the energetic component, so that $f_0 = f_0(v^2/2)$ with $v^2 = |\boldsymbol{v}|^2$. Notice that the special case $\boldsymbol{B}_0 = 0$ yields free transport for the hot particles, in the case of the non-Hamiltonian model ($\alpha = 0$). Conversely, the Hamiltonian model ($\alpha = 1$) retains the fluid velocity terms in the kinetic equation, even in the absence of the magnetic field ($\boldsymbol{B}_0 = 0$).

Notice that, although here we have chosen a Vlasov equilibrium of the form $f_0 = f_0(v^2/2)$, other more realistic choices are also available. For example, in actual hybrid simulations of the non-Hamiltonian PCS in fusion devices, toroidal symmetry is involved and the use of special equilibrium profiles becomes necessary [29]. Another example arises in reversed field pinch plasmas, in which finite Larmor radius effects allow for equilibria of the type $f_0 = f_0(\boldsymbol{x}, v^2) - \omega_c^{-1}\nabla f_0 \cdot \boldsymbol{v} \times \boldsymbol{B}$ (where $\omega_c = q_h B_0/m_h$) (see [11]). On the other hand, the aim here is not to enter into detailed features of particular fusion devices, but to provide insight into model differences. Therefore, we focus on distributions of the type $f_0 = f_0(v^2/2)$.

Assuming perturbations varying as $A_1 = \widetilde{A}_1 e^{i(\boldsymbol{k}\cdot\boldsymbol{x}-\omega t)}$ gives

$$\omega\widetilde{\boldsymbol{U}}_1 = \boldsymbol{k}\,\widetilde{\mathsf{p}}_1 + \int(\boldsymbol{k}\cdot\boldsymbol{v})\boldsymbol{v}\,\widetilde{f}_1\,\mathrm{d}^3\boldsymbol{v} + \boldsymbol{B}_0\times(\boldsymbol{k}\times\widetilde{\boldsymbol{B}}_1), \quad (33)$$

$$-\omega\widetilde{\boldsymbol{B}}_1 = (\boldsymbol{k}\cdot\boldsymbol{B}_0)\widetilde{\boldsymbol{U}}_1\,, \qquad \boldsymbol{k}\cdot\widetilde{\boldsymbol{U}}_1 = 0. \quad (34)$$

Dotting equation (33) by $\boldsymbol{k}$ and using equations (34) yields

$$\widetilde{\mathsf{p}}_1 = -\frac{1}{|\boldsymbol{k}|^2}\int(\boldsymbol{k}\cdot\boldsymbol{v})^2\,\widetilde{f}_1\,\mathrm{d}\boldsymbol{v} + \frac{1}{\omega}\,(\boldsymbol{k}\cdot\boldsymbol{B}_0)(\widetilde{\boldsymbol{U}}_1\cdot\boldsymbol{B}_0),$$

and the velocity equation becomes

$$\omega\widetilde{\boldsymbol{U}}_1 = -\int\left[\frac{(\boldsymbol{k}\cdot\boldsymbol{v})^2}{|\boldsymbol{k}|^2}\boldsymbol{k} - (\boldsymbol{k}\cdot\boldsymbol{v})\boldsymbol{v}\right]\widetilde{f}_1\,\mathrm{d}\boldsymbol{v} + \frac{1}{\omega}\,(\boldsymbol{k}\cdot\boldsymbol{B}_0)^2\,\widetilde{\boldsymbol{U}}_1 \quad (35)$$

or, upon rearranging the various terms,

$$\widetilde{\boldsymbol{U}}_1 = \frac{\omega}{(\omega^2 - \boldsymbol{k}\cdot\boldsymbol{B}_0)^2}\left[\boldsymbol{1} - \frac{\boldsymbol{k}\boldsymbol{k}}{|\boldsymbol{k}|^2}\right](\boldsymbol{k}\cdot\widetilde{\mathbb{P}}_1), \quad (36)$$

where $\widetilde{\mathbb{P}}_1 = \int\boldsymbol{v}\boldsymbol{v}\,\widetilde{f}_1\,\mathrm{d}^3\boldsymbol{v}$ and $\boldsymbol{1} - \boldsymbol{k}\boldsymbol{k}/|\boldsymbol{k}|^2$ projects transverse to $\boldsymbol{k}$.

It remains to express $\widetilde{f}_1$ in terms of $\widetilde{\boldsymbol{U}}_1$ in order to obtain the dispersion relation. This step is performed in section 3.3, but first the next section contains some relevant properties of the linearized equation of Vlasov kinetic moments.

3.2. Remarks on linearized moment dynamics

Before analyzing the linear dynamics, it is of interest to explore some roles played by the α and β terms. To this end it is useful to introduce equilibrium moments

$$\left(A_n^{(0)}\right)_{i_1 i_2\ldots i_n} = \int v_{i_1}\ldots v_{i_n}\,f_0\,\mathrm{d}^3\boldsymbol{v}.$$

since $f_0 = f_0(v^2/2)$, we notice that $A^{(0)}_{2n+1} = 0$. Then, equation (31) leads to the following conclusions about the equations of motion for the kinetic moments $A_k^{(1)} = \int v^k f_1\,\mathrm{d}^3\boldsymbol{v}$:

- the α-term (of the Hamiltonian model) contributes only to moments of even order $2n+2$ (e.g. the pressure tensor $\mathbb{P}_1$), i.e., the α-term does not contribute to the dynamics of odd-order moments;
- the β-term (of the non-Hamiltonian model) contributes only to moments of odd order $2n+1$ (e.g. the averaged momentum $\boldsymbol{K}_1$), i.e., the β-term does not contribute to the dynamics of even-order moments;
- the first three moments obey the equations

$$\partial_t n_1 + \nabla\cdot\boldsymbol{K}_1 = 0$$
$$\partial_t\boldsymbol{K}_1 + \nabla\cdot\mathbb{P}_1 - \boldsymbol{K}_1\times\boldsymbol{B}_0 = -\beta n_0\,\boldsymbol{U}_1\times\boldsymbol{B}_0$$
$$\partial_t\mathbb{P}_1 + \nabla\cdot A_3^{(1)} + \left[\widehat{B}_0, \mathbb{P}_1\right] = -2\alpha\Big((\mathbb{P}_0\cdot\nabla)\boldsymbol{U}_1 + ((\mathbb{P}_0\cdot\nabla)\boldsymbol{U}_1)^T\Big),$$

where $[\cdot,\cdot]$ denotes matrix commutator and we defined the hat operator by $\widehat{w}\boldsymbol{a} := \boldsymbol{w}\times\boldsymbol{a}$ (for any two vectors $\boldsymbol{w}$ and $\boldsymbol{a}$, so that $\widehat{w}_{ih} = -\epsilon_{ihk}w_k$ is an antisymmetric matrix).

Thus, there is no contribution of the α-term to the linearized fluid moments (i.e. zeroth and first-order moments) of the kinetic component: indeed, the α-term disappears in the linearized dynamics of the fluid closure for the hot particles. The α-term contributes only to the dynamics of perturbed moments at even order (e.g. the pressure tensor). On the other hand, the β-term contributes only to the dynamics of perturbed moments with odd order, e.g. it has a non-zero contribution to the first-order moment (which plays a crucial role in the CCS).

3.3. Solution of the linearized Vlasov equation

Now we solve the linearized kinetic equation (31) in terms of the fluid velocity $\boldsymbol{U}_1$. This is done by invoking the method of characteristics (integrating over orbits) as is standard in plasma physics texts (e.g. [13]) for the Maxwell–Vlasov system. Following this standard method yields the solution of the Vlasov equation in the form

$$f_1 = \int_{-\infty}^{t} f_0'\left(\alpha\nabla\boldsymbol{U}_1^* : \boldsymbol{v}^*\boldsymbol{v}^* - \beta\boldsymbol{U}_1^*\cdot\boldsymbol{v}^*\times\boldsymbol{B}_0\right)\mathrm{d}t^* + f_1(\boldsymbol{x}^*(-\infty), \boldsymbol{v}^*(-\infty), -\infty),$$

where f_0' means derivative of f_0 with respect to its argument ${v^*}^2/2$ and the variables $(\boldsymbol{x}^*(t^*), \boldsymbol{v}^*(t^*), t^*)$ satisfy

$$\dot{\boldsymbol{x}}^*(t^*) = \boldsymbol{v}^*(t^*), \qquad \dot{\boldsymbol{v}}^*(t^*) = \boldsymbol{v}^*(t^*)\times\boldsymbol{B}_0,$$

with $\boldsymbol{x}^*(t) = \boldsymbol{x}$, $\boldsymbol{v}^*(t) = \boldsymbol{v}$ and the dot indicating the derivative with respect to the evolution parameter t^*.

Then, upon introducing the notation $\omega_{B_0} = |\boldsymbol{B}_0|$ (i.e. the cyclotron frequency, upon restoring physical quantities) and the planar rotation

$$\mathcal{R}(\tau) = \exp(\tau\widehat{B}_0) = \begin{pmatrix}\cos(\omega_{B_0}\tau) & -\sin(\omega_{B_0}\tau) & 0\\ \sin(\omega_{B_0}\tau) & \cos(\omega_{B_0}\tau) & 0\\ 0 & 0 & 1\end{pmatrix}$$

and its antiderivative $A\mathcal{R}(\tau)$, we have

$$\boldsymbol{x}^* = A\mathcal{R}(\tau)\boldsymbol{v} + \omega_{B_0}^{-2}\boldsymbol{B}_0 \times \boldsymbol{v} + \boldsymbol{x},$$

together with $\boldsymbol{v}^* = \mathcal{R}(\tau)\boldsymbol{v}$ and $\tau = t^* - t$. Upon Fourier-transforming in the spatial variable, we obtain

$$\begin{aligned}\widetilde{f}_1 &= \int_{-\infty}^{0} f_0' \left(i\alpha(\boldsymbol{k}\cdot\boldsymbol{v}^*)(\widetilde{\boldsymbol{U}}_1\cdot\boldsymbol{v}^*) + \beta\widetilde{\boldsymbol{U}}_1\cdot\boldsymbol{B}_0\times\boldsymbol{v}^*\right) \\ &\quad\times e^{i(\boldsymbol{k}\cdot\boldsymbol{X}-\omega\tau)}\mathrm{d}\tau \\ &= \int_{-\infty}^{0} f_0' \left(i\alpha(\boldsymbol{k}\cdot\mathcal{R}(\tau)\boldsymbol{v})\widetilde{\boldsymbol{U}}_1 - \beta\boldsymbol{B}_0\times\widetilde{\boldsymbol{U}}_1\right)\cdot\mathcal{R}(\tau)\boldsymbol{v} \\ &\quad\times e^{i(\boldsymbol{k}\cdot\boldsymbol{X}-\omega\tau)}\mathrm{d}\tau,\end{aligned}$$

where $\boldsymbol{X} := \boldsymbol{x}^* - \boldsymbol{x}$ and recall $v_z^* = v_z$ and $z^*(\tau) = v_z\tau + z$, so that $\mathcal{R}\boldsymbol{B}_0 = \boldsymbol{B}_0$ and $(\mathcal{R}\widetilde{\boldsymbol{U}}_1)_z = \widetilde{U}_{1z}$. Thus, since $\mathcal{R}$ is a rotation,

$$\begin{aligned}\widetilde{f}_1 = \int_{-\infty}^{0} \frac{\partial f_0}{\partial \boldsymbol{v}}\cdot\Big(&i\alpha(\boldsymbol{k}\cdot\mathcal{R}(\tau)\boldsymbol{v})\mathcal{R}^T(\tau)\widetilde{\boldsymbol{U}}_1 \\ &-\beta\boldsymbol{B}_0\times\mathcal{R}^T(\tau)\widetilde{\boldsymbol{U}}_1\Big)\,\mathrm{e}^{\mathrm{i}(\boldsymbol{k}\cdot\boldsymbol{X}-\omega\tau)}\,\mathrm{d}\tau. \qquad (37)\end{aligned}$$

Finally, upon recalling the definition $\widehat{\boldsymbol{w}}\boldsymbol{a} := \boldsymbol{w}\times\boldsymbol{a}$ of hat operator, the velocity equation becomes

$$\begin{aligned}&\left(\omega^2 - (\boldsymbol{k}\cdot\boldsymbol{B}_0)^2\right)\widetilde{\boldsymbol{U}}_1 \\ &\quad= \omega\left[\boldsymbol{1} - \frac{\boldsymbol{k}\boldsymbol{k}}{|\boldsymbol{k}|^2}\right]\iint_{-\infty}^{0}(\boldsymbol{k}\cdot\boldsymbol{v})\left[\mathcal{R}\Big(i\alpha(\boldsymbol{k}\cdot\mathcal{R}\boldsymbol{v})\frac{\partial f_0}{\partial\boldsymbol{v}}\right. \\ &\qquad\left.+\beta\widehat{B}_0\frac{\partial f_0}{\partial\boldsymbol{v}}\Big)\cdot\widetilde{\boldsymbol{U}}_1\right]\boldsymbol{v}e^{i(\boldsymbol{k}\cdot\boldsymbol{X}-\omega\tau)}\,\mathrm{d}\tau\,\mathrm{d}\boldsymbol{v}. \qquad (38)\end{aligned}$$

and the dispersion relation is

$$\begin{aligned}\det\Big(&k^2\left((\boldsymbol{k}\cdot\boldsymbol{B}_0)^2-\omega^2\right)\boldsymbol{1} \\ &-\omega\widehat{k}^2\iint_{-\infty}^{0}(\boldsymbol{k}\cdot\boldsymbol{v})\,\boldsymbol{v}\left(i\alpha(\boldsymbol{k}\cdot\mathcal{R}\boldsymbol{v})\boldsymbol{1}+\beta\widehat{B}_0\right) \\ &\times\mathcal{R}\frac{\partial f_0}{\partial\boldsymbol{v}}e^{i(\boldsymbol{k}\cdot\boldsymbol{X}-\omega\tau)}\,\mathrm{d}\tau\,\mathrm{d}\boldsymbol{v}\Big) = 0. \qquad (39)\end{aligned}$$

At this point, one may write the general dispersion relation explicitly. However, we study the linearized system in two particular cases where $\boldsymbol{k}_\perp = 0$ and $k_z = 0$, which we turn to in the next sections.

4. Disturbances with $\boldsymbol{k}_\perp = 0$

Now we specialize the preceding results to the special case $\boldsymbol{k}_\perp = 0$, thus giving the dispersion relation for parallel propagating transverse disturbances with $\boldsymbol{k}\cdot\widetilde{\boldsymbol{E}}_1 = -\boldsymbol{k}\cdot\widetilde{\boldsymbol{U}}_1\times\boldsymbol{B}_0 = 0$.

4.1. Dispersion relation

After setting $\boldsymbol{k}_\perp = 0$ in equation (38) it is useful to compute the perturbed moment quantities $\widetilde{\boldsymbol{K}}_1$ and $\boldsymbol{k}\cdot\widetilde{\mathbb{P}}_1$. Notice that $\boldsymbol{k}_\perp = 0$ implies $k_z\widetilde{U}_{1z} = 0 \Rightarrow \widetilde{U}_{1z} = 0$. We compute $\widetilde{\boldsymbol{K}}_1$ by taking the first-order moment of (37). Upon integrating by parts and recalling $\mathcal{R}^T\boldsymbol{k} = \mathcal{R}\boldsymbol{k} = \boldsymbol{k}$, we have

$$\begin{aligned}\widetilde{\boldsymbol{K}}_1 &= \int \boldsymbol{v}\,\widetilde{f}_1(\boldsymbol{v})\,\mathrm{d}\boldsymbol{v} \\ &= \int \boldsymbol{v}\frac{\partial f_0}{\partial\boldsymbol{v}_\perp}\cdot\int_{-\infty}^{0}\Big(i\alpha k_z v_z\mathcal{R}^T(\tau)\widetilde{\boldsymbol{U}}_1 \\ &\quad-\beta\boldsymbol{B}_0\times\mathcal{R}^T(\tau)\widetilde{\boldsymbol{U}}_1\Big)\mathrm{e}^{\mathrm{i}(k_z v_z\tau-\omega\tau)}\,\mathrm{d}\tau\mathrm{d}\boldsymbol{v}_\perp\mathrm{d}v_z \\ &= -\int\int_{-\infty}^{0} f_0\Big(i\alpha k_z v_z\mathcal{R}^T(\tau)\widetilde{\boldsymbol{U}}_1 \\ &\quad-\beta\boldsymbol{B}_0\times\mathcal{R}^T(\tau)\widetilde{\boldsymbol{U}}_1\Big)\mathrm{e}^{\mathrm{i}(k_z v_z\tau-\omega\tau)}\,\mathrm{d}\tau\mathrm{d}\boldsymbol{v} \\ &= -\int\int_{-\infty}^{0} \bar{f}_0(v_z^2/2)\Big(i\alpha k_z v_z\mathcal{R}^T(\tau)\widetilde{\boldsymbol{U}}_1 \\ &\quad-\beta\boldsymbol{B}_0\times\mathcal{R}^T(\tau)\widetilde{\boldsymbol{U}}_1\Big)\mathrm{e}^{\mathrm{i}(k_z v_z\tau-\omega\tau)}\,\mathrm{d}\tau\mathrm{d}v_z.\end{aligned}$$

Hence,

$$\widetilde{K}_{1z} = 0.$$

The above relation means that the momentum perturbation $\widetilde{\boldsymbol{K}}_1$ is coplanar with $\widetilde{\boldsymbol{U}}_1$, i.e., $\widetilde{\boldsymbol{K}}_1\times\widetilde{\boldsymbol{U}}_1 = 0$ and therefore the density perturbation vanishes, since $\widetilde{n}_1 = -\boldsymbol{k}\cdot\widetilde{\boldsymbol{K}}_1/\omega \equiv 0$. Here, we have introduced the notation $\bar{f}_0(v_z^2/2) = \int f_0\,\mathrm{d}\boldsymbol{v}_\perp$. Notice that, by proceeding analogously, we have

$$\begin{aligned}\boldsymbol{k}\cdot\widetilde{\mathbb{P}}_1 = -\iint_{-\infty}^{0}&\bar{f}_0(v_z^2/2)\,k_z v_z\Big(i\alpha k_z v_z\mathcal{R}^T\widetilde{\boldsymbol{U}}_1 \\ &-\beta\boldsymbol{B}_0\times\mathcal{R}^T\widetilde{\boldsymbol{U}}_1\Big)\mathrm{e}^{\mathrm{i}(k_z v_z-\omega)\tau}\,\mathrm{d}\tau\mathrm{d}v_z.\end{aligned}$$

At this point one needs to compute the matrix integral

$$\mathcal{A} = \int_{-\infty}^{0}\mathrm{e}^{\mathrm{i}(k_z v_z-\omega)\tau}\mathcal{R}(\tau)\,\mathrm{d}\tau,$$

whose components are

$$\mathcal{A}_{11} = \mathcal{A}_{22} = -i\frac{k_z v_z-\omega}{(k_z v_z-\omega)^2-\omega_{B_0}^2}, \qquad (40)$$

$$\mathcal{A}_{12} = -\mathcal{A}_{21} = \frac{\omega_c}{(k_z v_z-\omega)^2-\omega_{B_0}^2}, \qquad (41)$$

$$\mathcal{A}_{33} = -\frac{i}{k_z v_z-\omega}.$$

In the above equations, the integrations are defined for $\mathrm{Im}(\omega) > 0$; following the standard procedure the solution is extended to the lower complex plane by analytical continuation. In conclusion, we have

$$\widetilde{\boldsymbol{K}}_1 = -\int\bar{f}_0(v_z^2/2)\left(i\alpha k_z v_z\boldsymbol{1}-\beta\widehat{B}_0\right)\mathcal{A}^T\widetilde{\boldsymbol{U}}_1\,\mathrm{d}v_z,$$

where we recall $\widehat{B}_{0ij} = -\epsilon_{ijk}B_{0k}$ and $(\mathcal{A}\widetilde{\boldsymbol{U}}_1)_z = 0$, so that $\widetilde{K}_{1z} = 0$. Similarly, we obtain

$$\boldsymbol{k}\cdot\widetilde{\mathbb{P}}_1 = -\int k_z v_z\bar{f}_0\left(i\alpha k_z v_z\boldsymbol{1}-\beta\widehat{B}_0\right)\mathcal{A}^T\widetilde{\boldsymbol{U}}_1\,\mathrm{d}v_z. \qquad (42)$$

Once the moment quantities $\widetilde{\boldsymbol{K}}_1$ and $\boldsymbol{k}\cdot\widetilde{\mathbb{P}}_1$ are written explicitly, one is ready to write the dispersion relation for the case $\boldsymbol{k}_\perp = 0$. Inserting the relation (42) into (36) yields

$$(k_z^2 b^2 - \omega^2)\widetilde{\boldsymbol{U}}_1 = \omega \int k_z v_z \bar{f}_0 \Big(i\alpha k_z v_z \mathcal{A}^T \widetilde{\boldsymbol{U}}_1 - \beta \boldsymbol{B}_0 \times \mathcal{A}^T \widetilde{\boldsymbol{U}}_1 \Big) \mathrm{d}v_z. \tag{43}$$

Notice, since $\widetilde{U}_{1z} = (\mathcal{A}^T \widetilde{\boldsymbol{U}}_1)_z = (\boldsymbol{B}_0 \times \mathcal{A}^T \widetilde{\boldsymbol{U}}_1)_z = 0$, this relation only possesses planar components.

At this point, direct algebraic computations on the above relation give the following dispersion relation:

$$D^\pm(\omega, k_z) := \omega^2 - k_z^2 v_A^2 + \omega(\alpha\omega \mp \omega_c) n_0 \left(1 + (\omega \mp \omega_c) \int_{-\infty}^{\infty} \frac{F}{k_z v_z - \omega \pm \omega_c} \mathrm{d}v_z \right) = 0, \tag{44}$$

where all physical constants have been restored: $\boldsymbol{B}_0 = B_0 \boldsymbol{e}_z$, $\omega_c = q_h B_0 / m_h$ is the cyclotron frequency of the energetic component, $v_A = B_0/\sqrt{\mu_0 \rho}$ indicates the Alfvén speed based on the constant equilibrium magnetic field B_0 and the constant bulk mass density ρ, and $F := \bar{f}_0 / n_0$ with $n_0 = \int_{-\infty}^{\infty} \bar{f}_0 dv_z$, so that n_0 is a dimensionless number indicating the ratio between the equilibrium mass density of the energetic component and that of the bulk component. (For details of this calculation see appendix B.)

4.2. Analysis of dispersion relation

Next we analyze the dispersion relation (44). Recall, if one sets $\alpha = 1$ in (44), one obtains the dispersion relation for the Hamiltonian model, whereas $\alpha = 0$ gives that for the non-Hamiltonian model. We will see that neglecting the terms that make the starting model Hamiltonian leads to important qualitative differences in the stability properties.

Some consequences of the dispersion relation (44) are immediate. In the absence of energetic particles ($n_0 = 0$), one recovers the dispersion relation $\omega = \pm v_A k_z$, describing Alfvén waves propagating along the z-direction. Next, assume 'cold hot' particles, i.e., the case where F is the Dirac delta function $\delta(v_z)$. In this case the hot particle contribution again vanishes, indicating that thermal effects are necessary to influence the Alfvén waves for both the Hamiltonian and non-Hamiltonian models.

To further analyze the two PCS' consider figure 1, where results are displayed from a numerical solution of the dispersion relation of (44) for the kappa distribution,

$$f_0^{(\kappa)} = \frac{n_0}{(\pi \kappa v_0^2)^{3/2}} \frac{\Gamma(\kappa+1)}{\Gamma(\kappa - 1/2)} \left(1 + \frac{v^2}{\kappa v_0^2} \right)^{-(\kappa+1)}. \tag{45}$$

Here v_0 reflects the thermal velocity $v_{\text{th}} = \sqrt{k_B T / m_h}$. Note, for large values of κ the κ-distribution is indistinguishable from the Maxwellian (see, e.g., [26]), and we have verified this by direct calculation by comparing the two for $\kappa = 50$. In figure 1, the imaginary part of the frequency, γ, is plotted against the wavenumber, k_z, suitably normalized, for the counter polarization, i.e., for D^+, which gives the weakest damping. In this figure we consider a hydrogen bulk plasma with a particle density of 10^{14} cm^{-3}, a magnetic field of 35 kG, and a alpha particle component with a temperature of 3.6 MeV and fractional density of $n_0 = 5 \times 10^{-3}$. This gives $v_0/v_A = 1.2$ and $\omega_c = 8.4 \times 10^7$ Hz. Since $n_0 \ll 1$, the real part of the frequency corresponds nearly to the Alfven wave, i.e., $\omega_r \approx k_z v_A$, so it is not plotted. Figure 1(*a*) depicts γ for the Hamiltonian PCS, while figure 1(*b*) shows the corresponding plot for the non-Hamiltonian PCS. The same behavior was found by varying n_0 within the range $n_0 \approx 10^{-3}$–10^{-1}, in agreement with the relations (48)–(50) below, obtained by the small growth rate expansion.

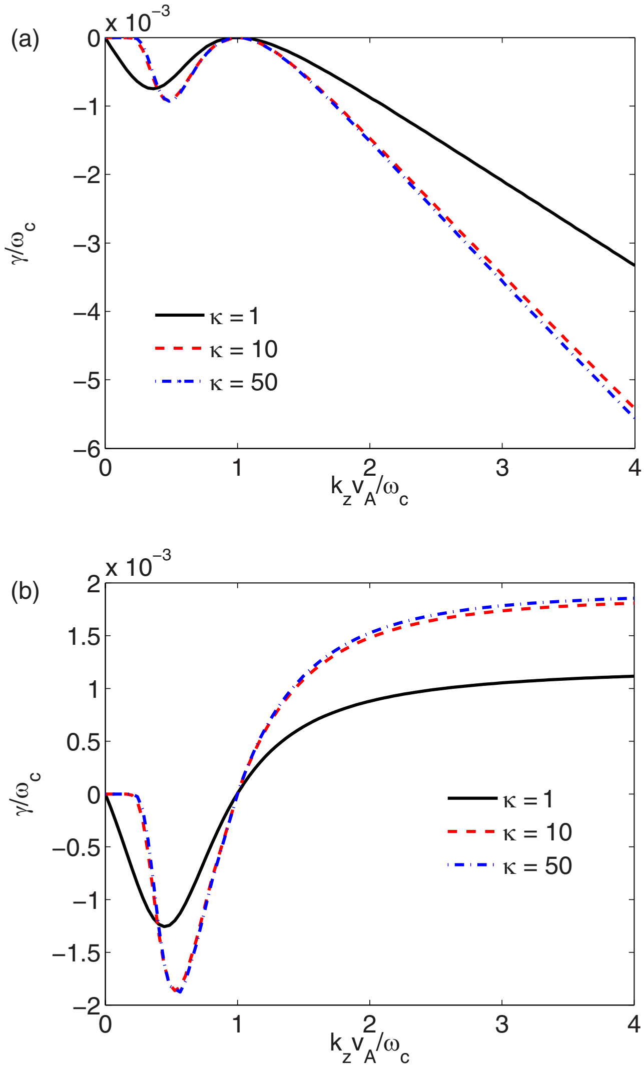

Figure 1. Plots of the normalized damping/growth rates versus wavenumber k_z for the PCS using the kappa distribution of equation (45) for different values of κ. Here $n_0 = 5 \times 10^{-3}$ and $v_0/v_A = 1.2$. (*a*) corresponds to the Hamiltonian PCS, which shows the expected damping, while (*b*) corresponds to the non-Hamiltonian PCS, which depicts the spurious instability for frequencies above ω_c.

The first observation to make is that both the Hamiltonian and usual non-Hamiltonian models have similar behaviors for low frequencies. This is to be expected, since the non-Hamiltonian pressure-coupling model was first developed to explore linear low frequency behavior. In fact, for example in [4], low frequency 'δW' type arguments were given that indicate stability in this frequency regime, which is consistent with the figures.

However, upon examination of figure 1 for larger values of k_z or $\omega_r \approx k_z v_A$, we see that figures 1(a) and (b) differ as ω_r approaches and exceeds ω_c. Most significantly, we see that the non-Hamiltonian PCS possess an instability for frequencies greater than ω_c, as is clearly evident in figure 1(b). Since the equilibrium we are considering has no available free energy, in either the bulk or in the hot particles, this instability must be nonphysical and reflects the lack of energy conservation in non-Hamiltonian PCS. For the Hamiltonian PCS displayed in figure 1(a), the system damps as expected. The hot particles provide Landau damping, in much the way one expects for electron Landau damping of Alfvén and whistler modes, with the mode at ω_c being undamped for one of the polarizations.

For $\kappa = 1$, it is easily shown by residue calculus that

$$\int_{-\infty}^{+\infty} \frac{F}{k_z v_z - \omega \pm \omega_c}\, \mathrm{d}v_z = -\frac{1}{i k_z v_0 + \omega \mp \omega_c},$$

where we recall $F = \bar{f}_0(v_z^2)/n_0$ and $\bar{f}_0(v_z^2)$ is obtained from equation (44) for $\kappa = 1$ (i.e. $f_0^{(1)}(v^2)$), upon integrating out the perpendicular components of the velocity. Thus (44) becomes

$$\omega^2 - k_z^2 v_A^2 + i n_0 \omega \frac{k_z v_0(\alpha\omega \mp \omega_c)}{i k_z v_0 + \omega \mp \omega_c} = 0.$$

From which one obtains for $n_0 \ll 1$, by expanding about $\omega = k_z v_A + i\gamma + \delta\omega_r$, the perturbed frequency

$$\gamma = -\frac{n_0}{2} \frac{k_z v_0(\alpha k_z v_A \mp \omega_c)(k_z v_A \mp \omega_c)}{k_z^2 v_0^2 + (k_z v_A \mp \omega_c)^2} \qquad (46)$$

$$\delta\omega_r = -\frac{n_0}{2} \frac{k_z^2 v_0^2(\alpha k_z v_A \mp \omega_c)}{k_z^2 v_0^2 + (k_z v_A \mp \omega_c)^2}. \qquad (47)$$

From (46) we see explicitly the spurious crossover to instability at ω_c observed in figure 1(b) that occurs for $\alpha = 0$. Similar, although progressively more complicated, formulae exist for higher values of κ (see, e.g., relation (117) in [26]), but we will not present these here.

Finally, we further explore the differences between the Hamiltonian and non-Hamiltonian models for arbitrary isotropic equilibria by examining the so-called small-γ approximation for each. Thus, we assume the resonant denominator of (44) gives rise to weak damping, and write $\omega = \omega_r + i\gamma$, $D = D_r^{\pm} + i D_i^{\pm}$, and then expand as usual to obtain

$$D_r^{\pm}(\omega_r, k_z) = 0, \qquad \gamma = -\frac{D_i^{\pm}(\omega_r, k_z)}{\partial D_r^{\pm}(\omega_r, k_z)/\partial\omega_r}. \qquad (48)$$

For $n_0 \ll 1$, $\partial D_r^{\pm}/\partial\omega_r \approx 2k_z v_A$, and, thus, $\gamma \approx -D_i^{\pm}(k v_A, k_z)/(2k v_A)$. Using the Plemelj relations we obtain the following form (44):

$$D_i^{\pm}(\omega_r, k_z) = \pi n_0(\alpha\omega_r \mp \omega_c)(\omega_r \mp \omega_c)\frac{\omega_r}{k_z} F\left(\frac{\omega_r \pm \omega_c}{k_z}\right). \qquad (49)$$

For the Hamiltonian PCS, $\alpha = 1$ and

$$D_i^{\pm} = \pi n_0(\omega_r \mp \omega_c)^2 \frac{\omega_r}{k_z} F\left(\frac{\omega_r \pm \omega_c}{k_z}\right), \qquad (50)$$

which indicates damping for both polarizations, except for the upper sign at $\omega_r = k_z v_A = \omega_c$ where the damping vanishes. However, upon setting $\alpha = 0$ we obtain for the non-Hamiltonian PCS, the following:

$$D_i^{\pm}(\omega_r, k_z) = \pi n_0\omega_c(\omega_c \mp \omega_r)\frac{\omega_r}{k} F\left(\frac{\omega_r \pm \omega_c}{k_z}\right), \qquad (51)$$

which reveals the strange nonphysical crossover to instability for one of the polarizations when $\omega_r > \omega_c$.

For the record, a calculation similar to that for the PCS gives for the CCS the dispersion relation

$$D^{\pm}(k_z, \omega) = \omega^2 - k_z^2 v_A^2 + \omega\omega_c n_0\left(\omega_c \int_{-\infty}^{+\infty} \frac{F}{k_z v_z - \omega \pm \omega_c}\, \mathrm{d}v_z \mp 1\right) \qquad (52)$$

whence we obtain for the Hamiltonian CCS, the following

$$D_i^{\pm}(\omega_r, k_z) = \pi n_0\omega_c^2 \frac{\omega_r}{k_z} F\left(\frac{\omega_r \pm \omega_c}{k_z}\right). \qquad (53)$$

Although (53) indicates a damping rate that is different from that of the Hamiltonian PCS, it does not possess the spurious instability possessed by the non-Hamiltonian PCS.

The damping rates indicated by (50), (51), and (53) have several features in common. First, for low frequencies, $\omega_r \ll \omega_c$, their intended regime, they all agree. Next, they all scale with F (as opposed to its derivative) which is appropriate for parallel propagating transverse waves for *all* isotropic equilibrium distribution functions (not just Maxwellians) [13]. For higher frequencies, (50), (51), and (53) disagree so it is useful to compare with a full kinetic theory with electrons, ions, and hot particle components. For cold electron and ion temperatures, only hot species contributes to the damping, and it is an elementary exercise to show that D_i for this case behaves precisely as (53), the result for the CCS. Thus, in this frequency range the CCS gives the best answer, although the Hamiltonian PCS may be reasonable. Clearly, the non-Hamiltonian result is unsatisfactory.

5. Disturbances with $k_z = 0$

This Section presents the dispersion relation for certain linear waves propagating transversely to the magnetic field. These modes are allowed by the Hamiltonian PCS model (27)–(29) (with $\nabla\cdot\boldsymbol{U} = 0$), while they are forbidden by the (incompressible) non-Hamiltonian variant (22)–(17). In particular, we study the special case $\widetilde{\boldsymbol{U}}_{1\perp} = 0$, which is consistent with the incompressibility relation $\boldsymbol{k}\cdot\widetilde{\boldsymbol{U}}_1 = 0$.

In order to find the dispersion relation, we specialize equation (36) by setting $k_z = 0$. In turn, this affects the Vlasov perturbation (37). Since $\widetilde{\boldsymbol{U}}_1 = \widetilde{U}_{1z}\boldsymbol{e}_z$ and

$$\boldsymbol{B}_0 \times \mathcal{R}^T(\tau)\widetilde{\boldsymbol{U}}_1 = \widetilde{U}_{1z}(\boldsymbol{B}_0 \times \mathcal{R}^T(\tau)\boldsymbol{e}_z) = \widetilde{U}_{1z}(\boldsymbol{B}_0 \times \boldsymbol{e}_z) = 0,$$

the Vlasov perturbation (37) becomes

$$\widetilde{f}_1 = i\alpha \int_{-\infty}^{0} (\boldsymbol{k}\cdot\mathcal{R}(\tau)\boldsymbol{v})\left(\frac{\partial f_0}{\partial\boldsymbol{v}}\cdot\mathcal{R}^T(\tau)\widetilde{\boldsymbol{U}}_1\right) e^{i(\boldsymbol{k}\cdot\boldsymbol{X} - \omega\tau)}\,\mathrm{d}\tau$$
$$= i\alpha\widetilde{U}_{1z}\frac{\partial f_0}{\partial v_z}\int_{-\infty}^{0} \boldsymbol{v}_\perp\cdot\mathcal{R}^T(\tau)\boldsymbol{k}\,\mathrm{e}^{\mathrm{i}(\boldsymbol{k}_\perp\cdot\boldsymbol{X}_\perp - \omega\tau)}\,\mathrm{d}\tau,$$

which shows how the non-Hamiltonian model ($\alpha = 0$) precludes the existence of transversal modes such that $\widetilde{\boldsymbol{U}}_{1\perp} = 0$. In what follows, we consider the Hamiltonian case by setting $\alpha = 1$.

Notice that, since $\boldsymbol{X}_\perp$ does not depend on v_z, the above expression yields $\widetilde{n}_1 = \int \widetilde{f}_1 \, \mathrm{d}^3 v = 0$. Therefore, the relation $\widetilde{n}_1 = \boldsymbol{k} \cdot \widetilde{\boldsymbol{K}}_1$ allows the case $\widetilde{\boldsymbol{K}}_1 = \widetilde{K}_{1z} \boldsymbol{e}_z$, where

$$\widetilde{K}_{1z} = i\alpha \widetilde{U}_{1z} \iint v_z \frac{\partial f_0}{\partial v_z} \int_{-\infty}^{0} \boldsymbol{v}_\perp \cdot \mathcal{R}^T(\tau) \boldsymbol{k}\, e^{i(\boldsymbol{k}_\perp \cdot \boldsymbol{X}_\perp - \omega\tau)} \times \mathrm{d}\tau \, \mathrm{d}\boldsymbol{v}_\perp \, \mathrm{d}v_z$$
$$= -i\alpha \widetilde{U}_{1z} \, \boldsymbol{k}_\perp \cdot \iiint_{-\infty}^{0} f_0 \, \mathcal{R}(\tau) \boldsymbol{v} \, \mathrm{e}^{\mathrm{i}(\boldsymbol{k}_\perp \cdot \boldsymbol{X}_\perp - \omega\tau)} \, \mathrm{d}\tau \, \mathrm{d}^3 v.$$

Then, combined with the velocity relation (36) and making use of the moment equation for $\boldsymbol{K}_1$ in section 3.2, the special case $\widetilde{\boldsymbol{K}}_{1\perp} = 0$ yields $\widetilde{U}_{1z} = \widetilde{K}_{1z}$ along with the dispersion relation

$$1 + i \iint_{-\infty}^{0} (\boldsymbol{k}_\perp \cdot \mathcal{R}(\tau) \boldsymbol{v}) \, f_0 \, e^{i(\boldsymbol{k}_\perp \cdot \boldsymbol{X}_\perp - \omega\tau)} \, \mathrm{d}\tau \, \mathrm{d}^3 v = 0.$$

This is an expected Bessel function type of dispersion relation and its detailed study is left for future work.

6. Summary and conclusions

After a review of hybrid kinetic-MHD models, we presented a comparative study of Hamiltonian and non-Hamiltonian PCSs, where the latter suffer by not exactly conserving energy. In particular, the two models were compared from the point of view of linear stability and their dispersion relations were presented and analyzed. The special cases of pure parallel and perpendicular wave propagation were considered.

Upon considering isotropic equilibria for the hot component, it was shown that the non-Hamiltonian PCS possesses an instability absent in its Hamiltonian variant and in the CCS, which is also Hamiltonian. We argued that the instability emerging in the non-Hamiltonian model is not physically viable. Extensive investigation of the dispersion relation will be considered in future work.

Although the unstable mode is of large frequency and thus outside the original intent of the PCS models, which were developed to describe low-frequency behavior, their presence would suggest results obtained from non-Hamiltonian PCS models extended into this regime should be viewed with caution. Even if some artifice, numerical or other, were used to suppress the unphysical linear instability, nonlinear coupling could give rise to differences in their turbulent transport behavior.

Acknowledgments

CT is indebted with J Carrillo, P Degond, D D Holm, G Lapenta and C Sovinec for several interesting discussions. Partial support by the Institute of Mathematics and its Applications Grant No. SGS27/13 is greatly acknowledged. P J M gratefully acknowledges stimulating conversations with B Breizman, C-Z Cheng, C W Horton, F Pegoraro and F Waelbroeck. His research was supported by the US Department of Energy Contract No. DE-FG05-80ET-53088. ET acknowledges financial support from the Agence Nationale de la Recherche (ANR GYPSI) and from the CNRS PEPS project GEOPLASMA.

Appendix A. Poisson brackets for Hamiltonian hybrid MHD models

A Hamiltonian system is a dynamical system generated by a given Hamiltonian (total energy) and a Poisson bracket in the form $\partial\Psi/\partial t = \{\Psi, H\}$, where Ψ denotes the set of dynamical variables. The Poisson bracket $\{\cdot, \cdot\}$ must be a bilinear, antisymmetric operator defined on the space of function(al)s. In addition it must satisfy he Leibniz property

$$\{FG, H\} = G\{F, H\} + F\{G, H\}$$

as well as the Jacobi identity

$$\{\{F, G\}, H\} + \{\{H, F\}, G\} + \{\{G, H\}, F\} = 0.$$

The Leibniz property, bilinearity and antisymmetry are easily built into the generic form of the Poisson bracket, but the proof of the Jacobi identity may require some effort. (See [16–19] for review and the appendix of [22] for a particularly onerous direct proof.) Such Poisson brackets need not have the canonical form of conventional field theories and may possess degeneracy—because of this they were called noncanonical in [21].

The Poisson brackets for the Hamiltonian models of the present paper were given in [31], where it was also shown how they may be used to formulate new hybrid MHD models that conserve energy exactly. Indeed, while exact conservation of (18) is guaranteed for the CCS model (14)–(17) by its noncanonical Poisson bracket

$$\begin{aligned}
\{F, G\}_{CCS} = & \int \boldsymbol{m} \cdot \left[\frac{\delta F}{\delta \boldsymbol{m}}, \frac{\delta G}{\delta \boldsymbol{m}}\right] \mathrm{d}^3\boldsymbol{x} \\
& - \int \rho \left(\frac{\delta F}{\delta \boldsymbol{m}} \cdot \nabla \frac{\delta G}{\delta \rho} - \frac{\delta G}{\delta \boldsymbol{m}} \cdot \nabla \frac{\delta F}{\delta \rho}\right) \mathrm{d}^3\boldsymbol{x} \\
& + q_h \int f \, \boldsymbol{B} \cdot \left(\frac{\delta F}{\delta \boldsymbol{m}} \times \frac{\delta G}{\delta \boldsymbol{m}} \right. \\
& \left. - \frac{\delta F}{\delta \boldsymbol{m}} \times \frac{\partial}{\partial \boldsymbol{p}} \frac{\delta G}{\delta f} + \frac{\delta G}{\delta \boldsymbol{m}} \times \frac{\partial}{\partial \boldsymbol{p}} \frac{\delta F}{\delta f}\right) \mathrm{d}^3\boldsymbol{x} \, \mathrm{d}^3\boldsymbol{p} \\
& + \int f \left(\left\{ \frac{\delta F}{\delta f}, \frac{\delta G}{\delta f} \right\} \right. \\
& \left. + q_h \boldsymbol{B} \cdot \frac{\partial}{\partial \boldsymbol{p}} \frac{\delta F}{\delta f} \times \frac{\partial}{\partial \boldsymbol{p}} \frac{\delta G}{\delta f} \right) \mathrm{d}^3\boldsymbol{x} \, \mathrm{d}^3\boldsymbol{p} \\
& + \int \boldsymbol{B} \cdot \left(\frac{\delta F}{\delta \boldsymbol{m}} \times \nabla \times \frac{\delta G}{\delta \boldsymbol{B}} - \frac{\delta G}{\delta \boldsymbol{m}} \times \nabla \times \frac{\delta F}{\delta \boldsymbol{B}} \right) \mathrm{d}^3\boldsymbol{x},
\end{aligned} \quad \text{(A1)}$$

the PCS models available in the literature fail to conserve energy exactly. For the Hamiltonian PCS (HPCS) (27)–(29), exact conservation of (14)–(17) follows from the Poisson bracket

$$\{F,G\}_{HPCS} = \int \boldsymbol{M}\cdot\left[\frac{\delta F}{\delta \boldsymbol{M}},\frac{\delta G}{\delta \boldsymbol{M}}\right]\mathrm{d}^3\boldsymbol{x}$$
$$-\int \rho\left(\frac{\delta F}{\delta \boldsymbol{M}}\cdot\nabla\frac{\delta G}{\delta \rho}-\frac{\delta G}{\delta \boldsymbol{M}}\cdot\nabla\frac{\delta F}{\delta \rho}\right)\mathrm{d}^3\boldsymbol{x}$$
$$+\int f\left(\left\{\frac{\delta F}{\delta f},\frac{\delta G}{\delta f}\right\}\right.$$
$$\left.+q_h\boldsymbol{B}\cdot\frac{\partial}{\partial \boldsymbol{p}}\frac{\delta F}{\delta f}\times\frac{\partial}{\partial \boldsymbol{p}}\frac{\delta G}{\delta f}\right)\mathrm{d}^3\boldsymbol{x}\,\mathrm{d}^3\boldsymbol{p}$$
$$+\int f\left(\left\{\frac{\delta F}{\delta f},\boldsymbol{p}\cdot\frac{\delta G}{\delta \boldsymbol{M}}\right\}-\left\{\frac{\delta G}{\delta f},\boldsymbol{p}\cdot\frac{\delta F}{\delta \boldsymbol{M}}\right\}\right)\mathrm{d}^3\boldsymbol{x}\,\mathrm{d}^3\boldsymbol{p}$$
$$+\int \boldsymbol{B}\cdot\left(\frac{\delta F}{\delta \boldsymbol{M}}\times\nabla\times\frac{\delta G}{\delta \boldsymbol{B}}-\frac{\delta G}{\delta \boldsymbol{M}}\times\nabla\times\frac{\delta F}{\delta \boldsymbol{B}}\right)\mathrm{d}^3\boldsymbol{x}. \tag{A2}$$

In the above formulas, $[\boldsymbol{X},\boldsymbol{Y}] := -(\boldsymbol{X}\cdot\nabla)\boldsymbol{Y}+(\boldsymbol{Y}\cdot\nabla)\boldsymbol{X}$ is minus the commutator on vector fields. The proof that the above bilinear, antisymmetric operators are indeed Poisson brackets (satisfying Leibniz and Jacobi) can be carried out by explicit verification. However, upon recognizing that these brackets are composed of terms of the original bracket of MHD [21] and that of the Maxwell–Vlasov system [14, 15, 19, 20], together with later work on the two-fluid system [27, 28], it is not difficult to ascertain the validity of the Jacobi identity.

Alternatively, one can begin with an action principle and derive the Poisson brackets, thereby ensuring the Jacobi identity. Such a Lagrangian formulation of the PCS equations (27)–(29) was given in [10]. We remark also that an action principle derivation of a linearized PCS model was presented in [2].

Appendix B. Derivation of dispersion relation for $k_\perp = 0$

This appendix contains the main steps leading to the dispersion relation (44). The starting point is the observation that $\widetilde{U}_{1z} = (\mathcal{A}^T\widetilde{\boldsymbol{U}}_1)_z = (\boldsymbol{B}_0\times\mathcal{A}^T\widetilde{\boldsymbol{U}}_1)_z = 0$ forces relation (43) to possess only planar components. Then, one can write the dispersion relation as

$$\left(\frac{\omega^2-k_z^2v_A^2}{\omega}-\int k_z\frac{\partial\bar{f}_0}{\partial v_z}\left(i\alpha k_z v_z\mathcal{A}_{11}+\beta v_A\mathcal{A}_{12}\right)\mathrm{d}v_z\right)^2$$
$$=\left(\int k_z\frac{\partial\bar{f}_0}{\partial v_z}\left(i\alpha k_z v_z\mathcal{A}_{12}+\beta v_A\mathcal{A}_{11}\right)\mathrm{d}v_z\right)^2,$$

where we recall the definitions (40)–(41). (Notice that $\bar{f}_0$ denotes the distribution function divided by the constant bulk particle density). Then, after some computations and upon restoring physical constants, one is led to

$$\frac{\omega^2-k_z^2v_A^2}{\omega}+\alpha\int_{-\infty}^{\infty}\frac{(k_zv_z)^2\bar{f}_0}{k_zv_z-\omega\pm\omega_c}\mathrm{d}v_z$$
$$=\pm\beta\omega_c\int_{-\infty}^{\infty}\frac{k_zv_z\bar{f}_0}{k_zv_z-\omega\pm\omega_c}\mathrm{d}v_z. \tag{B1}$$

The integrals of (B1) are then rearranged as follows:

$$\int_{-\infty}^{\infty}\frac{k_z^2v_z^2\bar{f}_0}{k_zv_z-\omega\pm\omega_c}\mathrm{d}v_z$$
$$=(\omega\mp\omega_c)\left(n_0+(\omega\mp\omega_c)\int_{-\infty}^{\infty}\frac{\bar{f}_0}{k_zv_z-\omega\pm\omega_c}\mathrm{d}v_z\right)$$
$$\int_{-\infty}^{\infty}\frac{\omega_ck_zv_z\bar{f}_0}{k_zv_z-\omega\pm\omega_c}\mathrm{d}v_z$$
$$=\omega_c\left(n_0+(\omega\mp\omega_c)\int_{-\infty}^{\infty}\frac{\bar{f}_0}{k_zv_z-\omega\pm\omega_c}\mathrm{d}v_z\right).$$

Finally, upon recalling that $\beta = 1-\alpha$, we write the dispersion relation as

$$\frac{\omega^2-k_z^2v_A^2}{\omega}=\left(\pm\,\omega_c(1-\alpha)-\alpha(\omega\mp\omega_c)\right)$$
$$\times\left(n_0+(\omega\mp\omega_c)\int_{-\infty}^{\infty}\frac{\bar{f}_0}{k_zv_z-\omega\pm\omega_c}\mathrm{d}v_z\right),$$

which eventually reduces to (44).

References

[1] Belova E V, Denton R E and Chan A A 1997 Hybrid simulations of the effects of energetic particles on low-frequency MHD waves *J. Comput. Phys.* **136** 324–36

[2] Brizard A 1994 Eulerian action principles for linearized reduced dynamical equations *Phys. Plasmas* **1** 2460–72

[3] Chen Y, White R B, Fu G-Y and Nazikian R 1999 Numerical study of the nonlinear evolution of toroidicity-induced Alfvén eigenmodes *Phys. Plasmas* **6** 226–37

[4] Cheng C Z 1991 A kinetic-magnetohydrodynamic model for low-frequency phenomena *J. Geophys. Res.* **96** 21159–71

[5] Freidberg J P 1982 Ideal magnetohydrodynamic theory of magnetic fusion systems *Rev. Mod. Phys.* **54** 801–902

[6] Fu G Y *et al* 1996 Recent progress in linear, nonlinear studies of toroidal Alfvén eigenmodes *Proc. 16th Int. Conf. Plasma Physics and Controlled Nuclear Fusion Research (Montreal, Canada, 1996)* IAEA-FI-CN-64/D2-6

[7] Fu G Y and Park W 1995 Nonlinear hybrid simulation of the toroidicity-induced Alfvén eigenmode *Phys. Rev. Lett.* **74** 1594–6

[8] Fu G Y, Park W, Strauss H R, Breslau J, Chen J, Jardin S and Sugiyama L E 2006 Global hybrid simulations of energetic particle effects on the $n = 1$ mode in tokamaks: internal kink, fishbone instability *Phys. Plasmas* **13** 052517

[9] Holm D D, Marsden J E, Ratiu T S and Weinstein A 1985 Nonlinear stability of fluid and plasma equilibria *Phys. Rep.* **123** 1–116

[10] Holm D D and Tronci C 2012 Euler-Poincaré formulation of hybrid plasma models *Commun. Math. Sci.* **10** 191–222

[11] Kim C C 2008 Preliminary simulations of FLR effects on RFP tearing modes *J. Fusion Energy* **27** 61–4

[12] Kim C C, Sovinec C R and Parker S E 2004 Hybrid kinetic-MHD simulations in general geometry *Comput. Phys. Commun.* **164** 448–55

[13] Krall N A and Trivelpiece A W 1973 *Principles of Plasma Physics* (New York: McGraw-Hill)

[14] Marsden J E and Weinstein A 1982 The Hamiltonian structure of the Maxwell–Vlasov equations *Physica* D **4** 394–406

[15] Marsden J E, Weinstein A, Ratiu T, Schimd R and Spencer R G 1983 Hamiltonian systems with symmetry, coadjoint orbits, plasma physics *Atti Accad. Sci. Torino Cl. Sci. Fis. Mat. Natur.* **117** 289–340

[16] Morrison P J 2005 Hamiltonian and action principle formulations of plasma physics *Phys. Plasmas* **12** 058102

[17] Morrison P J 1998 Hamiltonian description of the ideal fluid *Rev. Mod. Phys.* **70** 467–521
[18] Morrison P J 2009 On Hamiltonian and action principle formulations of plasma dynamics *AIP Conf. Proc.* **1188** 329–44
[19] Morrison P J 1982 Poisson brackets for fluids and plasmas *AIP Conf. Proc.* **88** 13–46
[20] Morrison P J 1986 The Maxwell–Vlasov equations as a continuous Hamiltonian system *Phys. Lett.* A **80** 383–6
[21] Morrison P J and Greene J M 1980 Noncanonical Hamiltonian density formulation of hydrodynamics and ideal magnetohydrodynamics *Phys. Rev. Lett.* **45** 790–4
[22] Morrison P J 2013 A general theory for gauge-free lifting *Phys. Plasmas* **20** 012104
[23] Morrison P J, Tassi E and Tronci C 2014 Energy stability analysis for a hybrid fluid-kinetic plasma model *Nonlinear Physical Systems—Spectral Analysis, Stability and Bifurcations* ed O Kirillov and D Pelinovsky (New York: Wiley) (doi:10.1002/9781118577608.ch14)
[24] Park W, Belova E V, Fu G Y, Tang X Z, Strauss H R and Sugiyama L E 1999 Plasma simulation studies using multilevel physics models *Phys. Plasmas* **6** 1796–803
[25] Park W *et al* 1992 Three-dimensional hybrid gyrokinetic-magnetohydrodynamics simulation *Phys. Fluids* B **4** 2033–7
[26] Podesta J J 2004 Plasma dispersion function for the kappa distribution *NASA Report* NASA/CR–2004-212770
[27] Spencer R G 1982 The Hamiltonian structure of multi-species fluid electrodynamics *AIP Conf. Proc.* **88** 121–6
[28] Spencer R G and Kaufman A N 1982 Hamiltonian structure of two-fluid plasma dynamics *Phys. Rev. A* **25** 2437–9
[29] Takahashi R, Brennan D P and Kim C C 2009 Kinetic effects of energetic particles on resistive MHD stability *Phys. Rev. Lett.* **102** 135001
[30] Todo Y, Sato T, Watanabe K, Watanabe T H and Horiuchi R 1995 Magnetohydrodynamic Vlasov simulation of the toroidal Alfvén eigenmode *Phys. Plasmas* **2** 2711–6
[31] Tronci C 2010 Hamiltonian approach to hybrid plasma models *J. Phys. A: Math. Theor.* **43** 375501